Aspect Ratio Effects on Neoclassical Tearing Modes from Comparison Between DIII-D and NSTX

R.J. La Haye[1], R.J. Buttery[1], S.P. Gerhardt[2], S.A. Sabbagh[3], and D.P. Brennan[4]

[1]*General Atomics, PO Box 85608, San Diego, California 92186-5608, USA*
[2]*Princeton Plasma Physics Laboratory, PO Box 451, Princeton, New Jersey 08543 USA*
[3]*Columbia University, 2960 Broadway, New York, New York 10027-6900 USA*
[4]*University of Tulsa, 800 South Tucker Drive, Tulsa, Oklahoma 74104 USA*

Toroidicity in a tokamak makes the total magnetic field on a flux surface vary poloidally so that it is stronger on the inboard side and weaker on the outboard side. Drift is added to particle gyrations and a fraction of particles are trapped on the outboard side in magnetic mirrors formed due to the poloidal variation of the magnetic field.[1] A bootstrap current arises (carried by passing electrons) which is approximately proportional to the product of the trapped fraction and the electron pressure gradient.[2] Neoclassical tearing modes (NTMs) are destabilized and sustained by helically perturbed bootstrap currents.[3] At sufficiently high beta (ratio of volume averaged plasma pressure to magnetic field pressure), a linearly stable tearing mode if seeded by another MHD event can have the seed reinforced, a destabilizing effect that can lower the plasma magnetic energy. However, curvature effects, i.e. field line bending by the island, tend to raise the magnetic energy, a stabilizing effect;[4-8] this is often called the GGJ effect after the original authors. The destabilizing helically perturbed bootstrap current is counter-acted by a number of effects at small island size; this tends to make an NTM linearly stable and non-linearly unstable, i.e., metastable.[3]

All of the toroidal effects depend on aspect ratio R/a, i.e., how spherical a tokamak is. Here, R is the major radius of the plasma boundary surface about the magnetic axis and a is the minor radius. The closer R/a is to one, the greater the effect and as R/a goes to infinity, such effects cease to exist. While the GGJ effect is usually neglected at large aspect ratio,[3] time dependent modeling in the low aspect ratio device MAST confirmed its significance at low aspect ratio.[9-10] In this paper, experimental results are contrasted between the typical "high" aspect ratio DIII-D $(R/a = 2.7)$ and the low aspect ratio NSTX $(R/a = 1.4)$.

Experimental setup. Both DIII-D and NSTX are run with near balanced double null divertor shapes of similar minor radius (a≈0.6 m), elongation (κ≈2), triangularity (δ_u≈0.4 and δ_l ≈0.7) and cross sectional area (≈2 m^2). DIII-D has plasma current I_p=0.8 MA and toroidal magnetic field on axis B_{T0}=1.3 or 2.0 T to vary the safety factor at the 95% flux surface from q_{95}=4.3 to 6.9. NSTX has I_p=0.9 MA and B_{T0}=0.44 T for q_{95}=8.0. The key parameter at issue is the local $q=m/n$ rational surface inverse aspect ratio ε (where m and n are the poloidal and toroidal wave numbers). This enters into the bootstrap drive, the GGJ curvature effect, and the small island stabilizing effects. For typical large aspect ratio tokamaks such as DIII-D, ε is estimated as r/R_0 which comes from the dominant poloidal in/out asymmetry in B_T. Rigorously, toroidal effects come from the variation in total B which is used here for ε.

The experimental procedure in each device is: (1) raise beta in a high confinement H-mode to excite an *m/n*=2/1 mode, (2) "slowly" reduce neutral beam injection (NBI) power and thus beta, (3) stay in H-mode as power is reduced, (4) avoid the rotating *n*=1 mode locking to the resistive wall as torque is reduced with less NBI, and (5) reach the marginal point for self-stabilization, i.e., removal of the metastable parameter space. DIII-D had to use gas puffing to stay in H-mode, otherwise, an H to L transition occurred and beta rapidly collapsed and profiles changed quickly. NSTX developed a reproducible *n*=1 onset condition using modest *Li* evaporation and mode locking was avoided by using both *n*=1 and *n*=3 error field correction.

DIII-D exhibits large hysteresis in beta between *n*=1 NTM onset (and saturation) and the marginal point for self-stabilization. This is shown in Fig. 1 for a discharge in which the *m/n*=2/1 mode is excited. NSTX exhibits little hysteresis. This is shown in Fig. 2 for the *m/n*=2/1 mode which saturates and is here closely followed by a single step down of NBI power. Absent small island effects, the magnitude of the NTM $|\tilde{B}_\theta|$ should scale as β_θ^2; this is normalized in Figs. 1 and 2 at the start of the power (and beta) reduction.

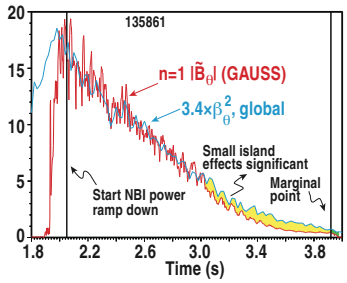

Fig. 1. $3.4 \times \beta_\theta^2$ and *n=1* $|\tilde{B}_\theta|$ in DIII-D vs time for an *m/n*=2/1 excited mode. The start of the NBI rampdown is noted which lowers global β_θ^2.

For an island of full width w, the island growth rate is given by the Modified Rutherford Equation (MRE),[11-12]

$$\frac{\tau_R}{r}\frac{dw}{dt} = \Delta' r + C_R \frac{rD_R}{w} + \varepsilon^{1/2}\frac{rL_q}{L_{pe}}\beta_{\theta e}\left[\frac{1}{w} - \frac{w_{small}^2}{3w^3}\right] \quad . \quad (1)$$

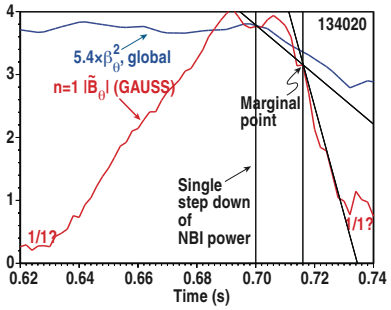

Fig. 2. Same as Fig. 1, but for NSTX *m/n*=2/1 mode. The multiplier on global β_θ^2 is adjusted to match *n=1* $|\tilde{B}_\theta|$ at the start of NBI reduction.

Here Δ' (in m^{-1}) is the classical tearing index and $C_R rD_R/w$ is the GGJ effect of assumed good average magnetic field curvature with dimensionless D_R the "resistive interchange parameter". To leading order in inverse aspect ratio at the rational surface, $D_R \approx -(q^2-1)(L_q^2/rL_p)\beta$ where L_q is the radial magnetic shear length, L_p is the total pressure gradient scale length, and $\beta = 2\mu_o p/B_{T0}^2$ with p the local total pressure. C_R= Θ(1) is a constant of proportionality which can be modified by finite aspect ratio effects. The destabilizing bootstrap current drive term in (1) is $\varepsilon^{1/2}\left(rL_q/L_{pe}w\right)\beta_{\theta e}$ where L_{pe}=(-p_e/dp_e/dR) and $\beta_{\theta e} \equiv 2\mu_o p_e/B_\theta^2$ is the local electron beta poloidal. Finally, all of small island stabilizing effects[13-14] are lumped together as w_{small}.

Marginal island width scaling. The *n*=1 data from DIII-D and NSTX for full marginal island width at the outboard midplane versus ion banana width are shown in Fig. 3. NSTX alone has a ratio of marginal island width to ion banana width of (3.02±0.40). The three different *n*=1 DIII-D cases do not individually have enough data to separately correlate.

However, two of the three DIII-D cases (blue 3.0 and 2.8 in Fig. 3) overlap the NSTX data, while a third case in which q=2/1 is closer to the magnetic axis, has a lower ratio of 1.80±0.09 for its three data points. Error bars for an NSTX case and two different 2/1 DIII-D cases to be analyzed in more detail are added in Fig. 3. The ratio of the marginal island width to the ion banana width is well correlated with $\varepsilon^{1/2}$ as shown in Fig. 4.

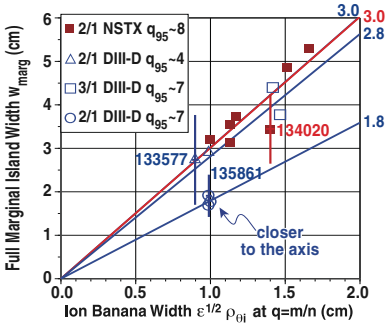

Fig. 3. Full marginal island width at outboard midplane $q=m/n$ vs ion banana width.

MRE balance as a method to evaluate the importance of the curvature effect. The DIII-D and NSTX cases at the marginal point are balanced with the destabilizing helically perturbed bootstrap current (counter-acted by the small island effects) just cancelled by the stabilizing sum of the classical tearing parameter (assumed stabilizing, i.e. negative) and the stabilizing effect of good magnetic field curvature (the GGJ effect). All DIII-D and NSTX cases are evaluated at the marginal point using equation (1) with the bracket set for $w_{small}=w_{marg}$. The inferred sum of the Δ' and curvature terms versus safety factor q_{95} is shown in Fig. 5. The m/n=2/1 mode in DIII-D shows greater stability at larger q_{95}. In contrast to DIII-D, the NSTX 2/1 data at the marginal point, all at about the same q_{95}, show a wide variation in Fig. 5. A hidden variable is clearly indicated. We look for this in the variation of the curvature term as seen in Fig. 6. There is a good correlation for NSTX with the curvature parameter rD_R/w. The linear fit (not forced through zero) extrapolates to about 0 at rD_R/w=0. This suggests that $\Delta' r \approx 0.0 \pm 0.4$ to the one sigma of the fit and that the curvature term is the dominant stabilizing effect that balances the helically perturbed bootstrap term (with small island effects). This explains the relatively little hysteresis in β in NSTX between the saturated balance before NBI stepdown and the marginal point shortly after stepdown; if the curvature term $\propto \beta$ and the bootstrap term $\propto \beta_{\theta e}$ scale together and are delicately balanced, with $\Delta' r$ "small," there is little difference between these two operating points. In contrast to NSTX, the curvature parameter in DIII-D for all three cases is much smaller as also seen in Fig. 6. Thus the stabilizing term in DIII-D is dominated by negative Δ' and a large hysteresis in β occurs.

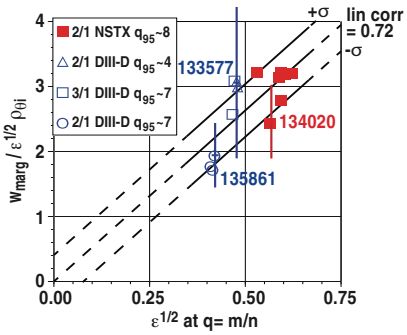

Fig. 4. Ratio of the marginal island width to the ion banana width vs square root of the inverse aspect ratio.

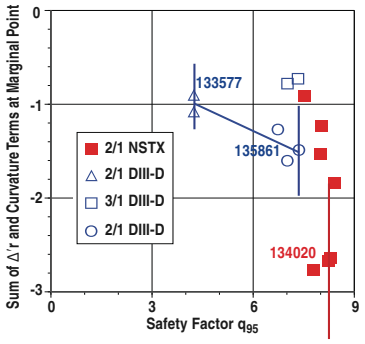

Fig.5. Sum of the Δ' and GGJ terms (from balance with the helically perturbed bootstrap term evaluated at the marginal point) versus safety factor q_{95}.

NIMROD stability calculations. The relative importance of the stabilizing curvature can be confirmed by the NIMROD resistive MHD stability code. MHD equilibrium reconstructions for typical m/n=2/1 cases are used as inputs. NIMROD[15] calculates the effective m/n=2/1 mode bootstrap drive coefficient D_{nc} in full shaped geometry using the simplified bootstrap drive from the electron pressure only.[7] NIMROD also calculates the resistive interchange stability parameter in the full shaped geometry. The flux surface averaging for both is done on the original equilibria in a separate part of the code "fluxgrid" and is not looking at the time advance of the fields. The dimensionless form of the MRE with D_{nc} positive, and Δ^*, D_R and D_{pol} negative, is here taken as[6, 16]

$$\frac{k_0}{\eta^*}\frac{dw}{dt} = \left(\Delta^* + \frac{D_R}{w}\right) + \left(\frac{D_{nc}}{w} + \frac{D_{pol}}{w^3}\right) \quad , \qquad (2)$$

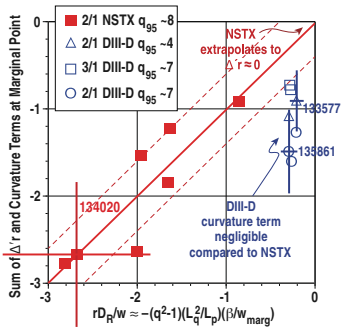

Fig. 6. Same as Fig. 5, but inferred sum of the stabilizing terms plotted versus the curvature parameter. The linear fit for NSTX and the $\pm 1\sigma$ certainties are overlaid.

where w is the full island width in normalized flux space, and D_{pol} allows an explicit small island stabilization to be included. We have gathered the stabilizing terms in the first set of parentheses, and the destabilizing bootstrap term counter-acted by small island effects in the second set. D_R from NIMROD is close to the large aspect ratio expansion analytic formula for NSTX, but NIMROD finds the D_R in DIII-D is 3~5 times a bigger effect than that of the expansion formula. However, curvature stabilization is found to still be relatively small in DIII-D. At the marginal point, we can assume the effective D_{pol}/w^3=-D_{nc}/3w. Then to gauge the stabilizing effect of the curvature relative to that of Δ', Eq. (2) yields at $\dot{w}=0$, $D_R/\Delta^* w = -1/\left(1+2D_{nc}/3D_R\right)$. The NSTX case #134020 is found by NIMROD to have a significant stabilizing curvature effect comparable to that of a negative Δ' (not directly calculated), but not dominant (5 to 1 as in the multi-shot fit of Fig. 6). The DIII-D cases are found to be Δ' dominated (3~6 times more stabilizing).

This work was supported in part by the U.S. Department of Energy under DE-FG02-04ER54698, DE-AC02-09CH11466, and DE-FG02-04ER54761. Thanks to the DIII-D and NSTX Teams.

[1] J. Wesson, *Tokamaks* 2nd edition, pp. 124-131, 166-168, (Clarendon Press-Oxford, 1997)
[2] O. Sauter *et al.* Phys. Plasmas **6**, 2834 (1999)
[3] R.J. La Haye Phys. Plasmas **13,** 055501 (2006)
[4] A.H. Glasser *et al*. Phys. Fluids **18,** 875 (1975)
[5] A.H. Glasser *et al*. Phys. Fluids **19,** 567 (1976)
[6] S.E. Kruger *et al*. Physics of Plasmas **5,** 455 (1998)
[7] C.C. Hegna, Phys. Plasmas **6,** 3980 (1999)
[8] H. Lütjens and J.F. Luciani, Phys. Plasmas **8,** 4267 (2001)
[9] R.J. Buttery *et al*. Phys. Rev. Lett. **88,** 125005 (2002)
[10] R.J. Buttery *et al*. Nucl. Fusion **44,** 1027 (2004)
[11] R.J. La Haye *et al*. Phys. Plasmas **17,** 056110 (2010)
[12] R.J. La Haye *et al*. and the DIII-D Team, Nucl. Fusion **51,** 053013 (2011)
[13] R. Fitzpatrick, Phys. Plasmas **2,** 825 (1995)
[14] F.L. Waelbroeck *et al*. Phys. Rev. Lett. **87,** 215003-1 (2001)
[15] C.R. Sovinec *et al*. Phys. Plasmas **10,** 1727 (2003)
[16] D.P. Brennan *et al*. Phys. Plasmas **9,** 2998 (2002)